Application of first-principles methods to binary and ternary alloy phase diagram predictions

1995 J. Phys.: Condens. Matter 7 3139

(http://iopscience.iop.org/0953-8984/7/16/009)

J. Phys.: Condens. Matter 7 (1995) 3139–3152. Printed in the UK

Application of first-principles methods to binary and ternary alloy phase diagram predictions

G Rubin†‡ and A Finel‡

† Institut für Mechanische Verfahrenstechnik und Mechanik, Universität Karlsruhe, D-76128 Karlsruhe, Postfach 6980, Germany

‡ Laboratoire de Physique des Solides, Office National d'Etudes et de Recherches Aerospatiales, BP 72, 92322 Chatillon Cédex, France

Received 7 November 1994, in final form 19 January 1995

Abstract. First-principles energy calculations, using the LMTO ASA method, have been performed for seven binary alloys (Ti–Al, Ti–Mo, Ti–Nb, Ti–W, Al–Mo, Al–Nb and Al–W). For the Ti–Mo system, our results lead to stability of the B32 ordered compounds, in contradiction with the experimental phase diagrams, which display a miscibility gap for the BCC lattice. Meanwhile, recent unpublished neutron diffraction measurements have been performed at a high temperature; they indicate the presence of a short-range order by a $\langle \frac{1}{2}\frac{1}{2}\frac{1}{2} \rangle$ q-vector, in perfect agreement with the stability of B32 at low temperatures. Secondly, we proceed to a cluster expansion, using the Connolly–Williams inversion scheme and the formation energies of a finite set of ordered configurations. We obtain, for each alloy, a set of cluster interactions and we test the transferability of this set to the formation energies of other ordered compounds. Finally, in order to calculate a ternary phase diagram (isotherm), the Connolly–Williams inversion scheme has been applied to a ternary formation energy. Then, we have calculated an isotherm of the Ti–Al–Nb system and found perfect agreement with the isotherm already calculated in an earlier publications, using a different approach.

1. Introduction

In the recent past, many first-principles energy calculations using the linear muffin-tin orbitals (LMTO), augmented sphere approximation (ASA) [1–4], within the local-density approximation (LDA) [5] have been realized. This method has proved its accuracy and ability to describe the structural stability of all the transition elements [6].

In the study of alloys, first-principles total-energy calculations have frequently been coupled with the so-called Connolly–Williams [7–9] inversion scheme. This inversion scheme is used to extract effective interaction parameters from total-energy calculations.

We have chosen to apply this analysis to the binary alloys that we have primarily considered in an earlier publication [10]: Ti–Al, Ti–Mo, Ti–Nb, Ti–W, Al–Mo, Al–Nb and Al–W. It will be very instructive to compare the calculated interaction parameters with the experimental segregation or ordering tendency observed in the experimental phase diagrams. We shall see that some surprises arise for the Ti–Mo and Ti–W systems. These results will be discussed in some detail. Then, we consider the Connolly–Williams method for ternary systems and calculate, with this form, an isothermal section of the Ti–Al–Nb system.

0953-8984/95/163139+14$19.50

2. Total energies and energies of formation

We have calculated total energies with Brillouin zone integrations based on 12^3, 14^3 and 16^3 k-points and observed a precision of 10^{-4} Ry with a 16^3 k-point mesh. The standard corrections to the ASA are included in our calculation and all the sphere radii are taken to be equal to the average Wigner–Seitz radius. Let us consider the seven binary alloys: Ti–Al, Ti–Mo, Ti–Nb, Ti–W, Al–Mo, Al–Nb and Al–W. For each of them, we have relaxed homogeneously the structure with regard to the crystalline parameter. All the fundamental phases of the BCC structure have been considered, with two other more complex phases: B11 (stoichiometry AB) and the two $C11_b$ (stoichiometry A_2B and AB_2) (figure 1).

Figure 1. Structures B11 and $C11_b$. The structures are projected on a (001) plane. The large circles correspond to sites on (00n) planes, and the small circles to sites in $(00n + \frac{1}{2})$ planes (n integer).

The total energies, as a function of the crystalline parameter, are shown in figure 2 for the pure elements, and in figure 3 for each binary alloy with the structure B2, B32 and DO_3. As we can see in figure 2, the equilibrium crystalline parameters of many pure elements are very close to each other. We present in table 1 the equilibrium crystalline parameters of the pure elements. The formation energy of any ordered compound is given by

$$E_{for} = E_{tot} - c_A E_A - c_B E_B. \tag{1}$$

Our results concerning the formation energies of the binary alloys with regard to the composition are presented in figure 4 and table 2. We note that these results indicate an ordering tendency in the Ti–Mo and Ti–W systems (see figures 4(b) and 4(d) respectively); this is in contradiction to the experimental phase diagrams (figure 5), which display miscibility gaps on the BCC lattice. We comment on that point in the next section.

Table 1. Total energies for the pure elements and corresponding crystalline parameters. $a_0 = 0.53$ Å is the Bohr radius.

Pure element	Total energy (Ryd for two atoms)	Equilibrium crystalline parameter (units of a_0)
Ti	−3409.5183	6.05 ± 0.05
Al	−968.5943	6
Mo	−16 182.1902	6
Nb	−15 266.5213	6.25
W	−64 538.5001	6

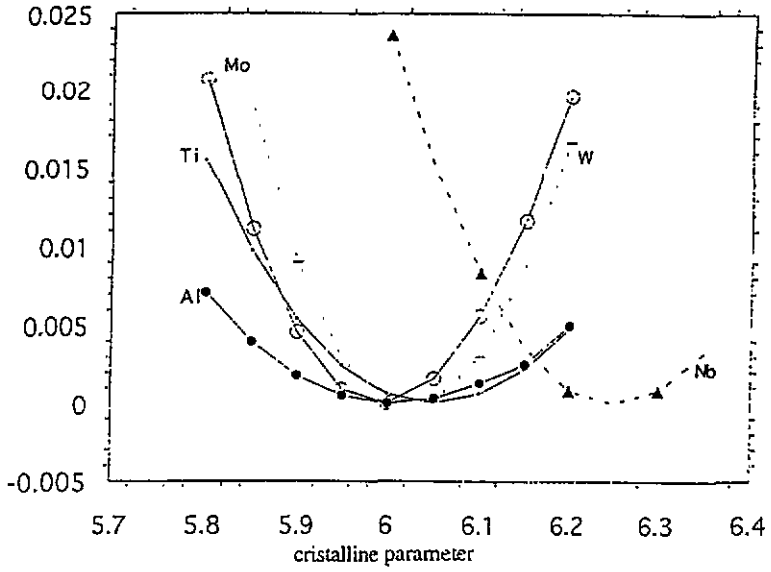

Figure 2. Total energies of pure elements. Units: y axis, Ryd for 2 atoms; x axis, Bohr radius.

3. Discussion of the LMTO ASA results

If we consider the Ti–Mo and Ti–W system results, the situation is very surprising. In these cases, a segregation tendency is observed experimentally (see figure 5) and we expect the formation energies of the ordered compounds to be positive. In fact, the formation energies of B2, B32 and the two $D0_3$ compound are definitely negative. This will lead to pair interactions relative to an ordering tendency.

How can we understand this situation? As a first step, we may wonder whether the experimental phase diagrams are really reliable. As a second step, we should try to reproduce our LMTO ASA results by other methods. Finally, we may wonder whether the effects that we have neglected, such as elastic relaxation, are responsible for the discrepancy between theory and experience. Let us examine each system more deeply.

3.1. The Ti–Mo system

A bibliographic study shows that the presence of the miscibility gap (top of the gap, 850 °C according to Murray [11]) is much debated. Three experimental studies have been realized which contradict the traditional phase diagram (see figure 5(*a*)).

First, through x-ray studies, Dupouy and Averbach [12] have shown the existence of strong short-range order in the BCC solid solution of the Ti–Mo system. Secondly, Morniroli and Gantois [13], also through x-ray studies, showed the same tendency to short-range order in the BCC solid solution for Ti–Mo and Ti–Nb. Finally, Gros [14] did not find the presence of a two-phase regime using microsonde and micrographic studies.

The existence of the miscibility gap is essentially due to the work of Terauchi *et al* [15], based on electrical resistive measurements.

What results are obtained from other electronic structure calculations methods? Recent calculations have been done by Pasturel [16] with the full potential (FP) LMTO method and give results quite similar to the LMTO ASA data, i.e. negative formation energies for the

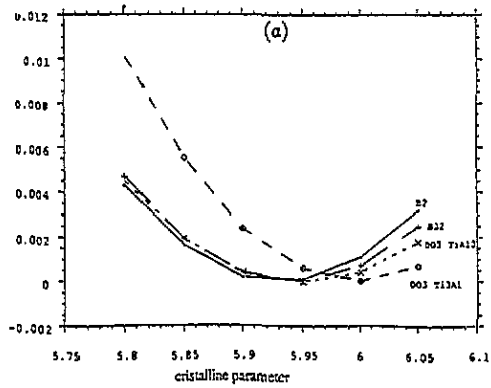

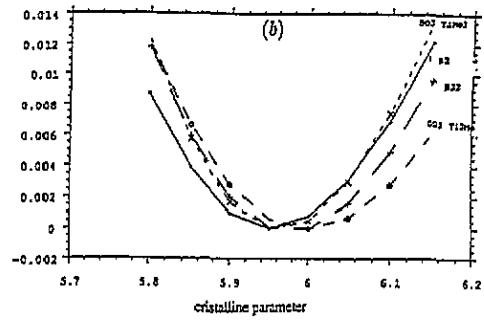

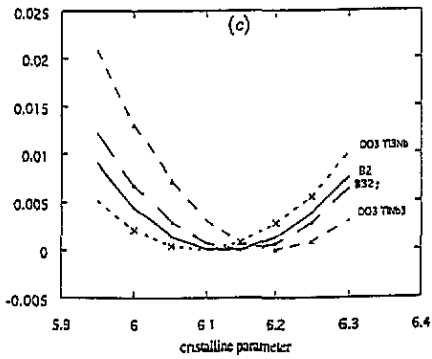

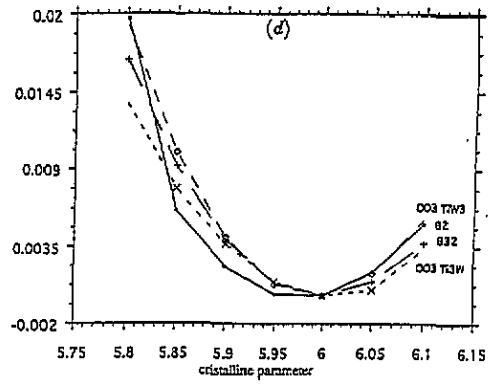

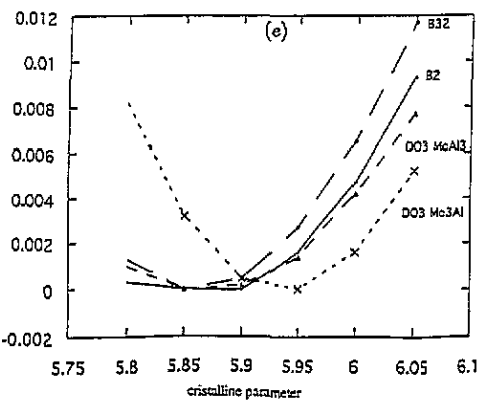

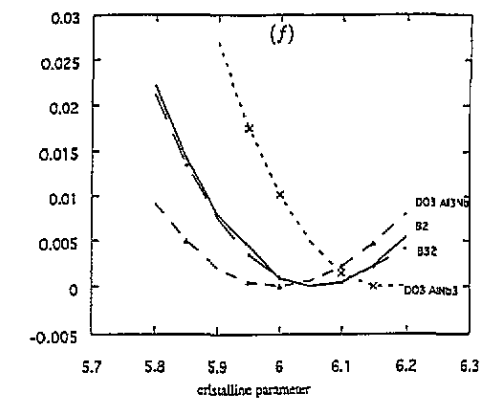

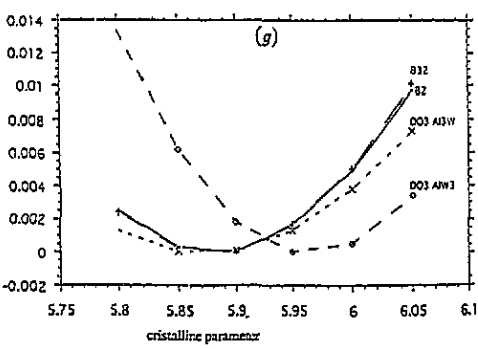

Figure 3. Total energies of (*a*) Ti–Al, (*b*) Ti–Mo, (*c*) Ti–Nb, (*d*) Ti–W, (*e*) Al–Mo, (*f*) Al–Nb, and (*g*) Al–W. Units: *y* axis, Ryd for 2 atoms; *x* axis; Bohr radius.

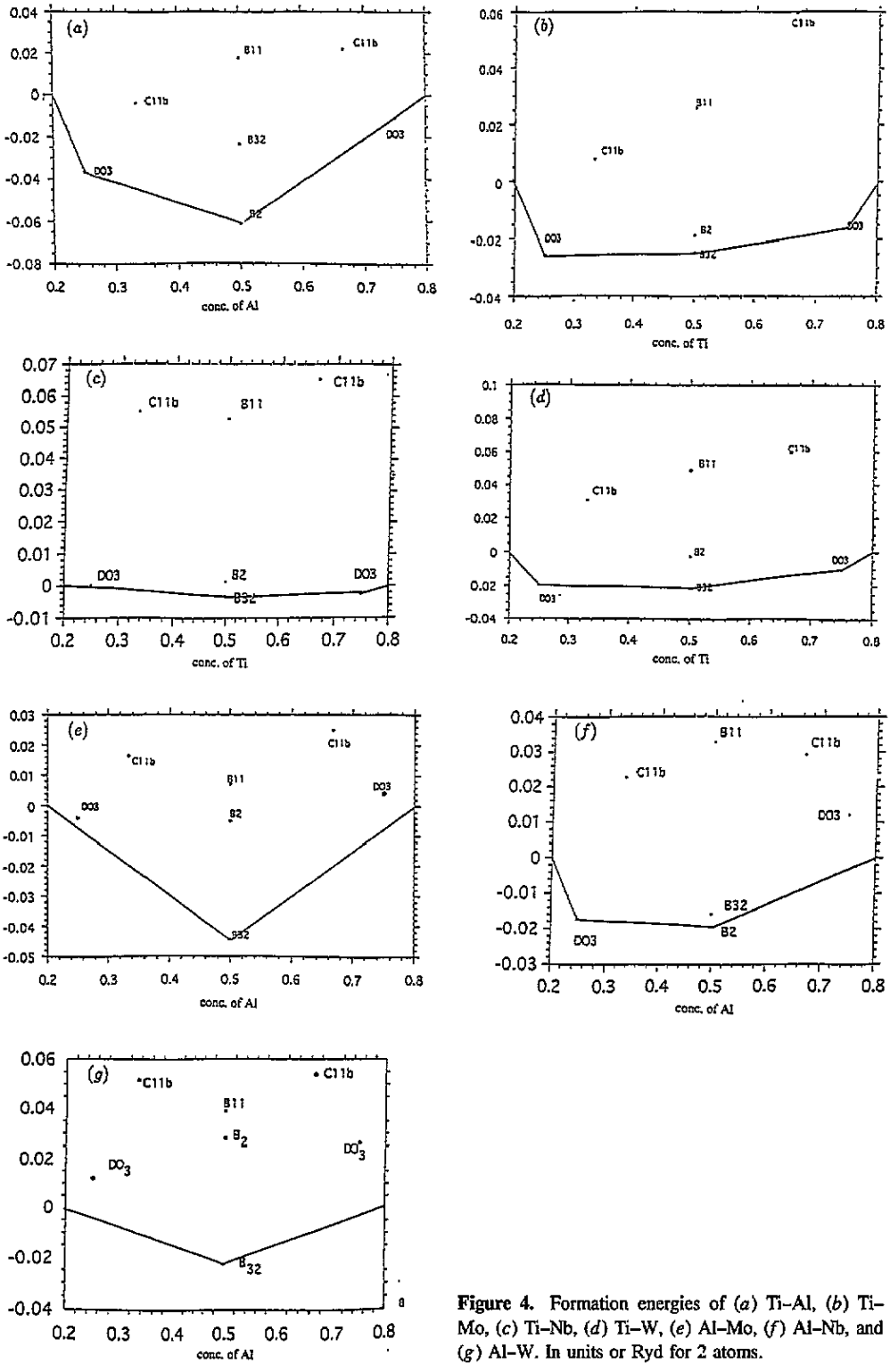

Figure 4. Formation energies of (*a*) Ti–Al, (*b*) Ti–Mo, (*c*) Ti–Nb, (*d*) Ti–W, (*e*) Al–Mo, (*f*) Al–Nb, and (*g*) Al–W. In units or Ryd for 2 atoms.

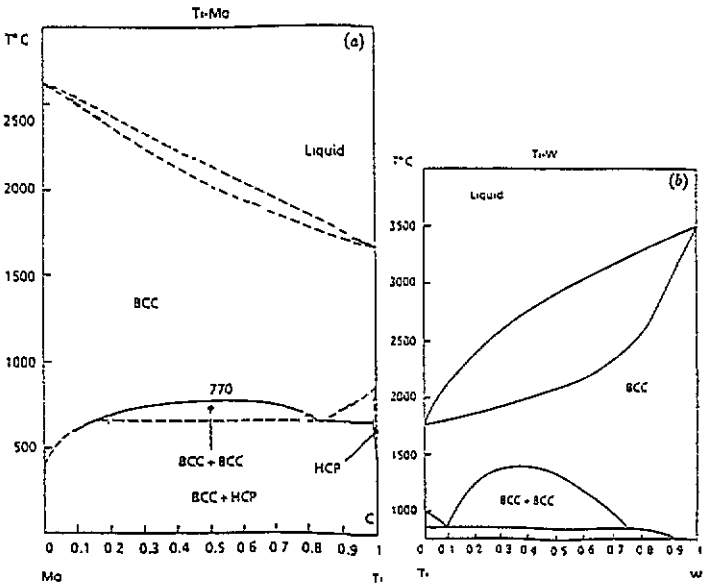

Figure 5. Experimental phase diagrams of Ti–Mo and Ti–W.

Table 2. Formation energies E_{for} for the seven alloys.

	E_{for} (Ryd for two atoms)						
	Ti–Al	Ti–Mo	Ti–Nb	Ti–W	Al–Mo	Al–Nb	Al–W
Pure A	0.0	0.0	0.0	0.0	0.0	0.0	0.0
Pure B	0.0	0.0	0.0	0.0	0.0	0.0	0.0
B2	−0.0612	−0.0188	0.0012	−0.0025	−0.0050	−0.0196	0.0282
B32	−0.0235	−0.0245	−0.0032	−0.0214	−0.0445	−0.0159	−0.0228
$D0_3$ (1)	−0.0107	−0.0163	−0.0025	−0.0102	0.0053	0.0117	0.0254
	($TiAl_3$)	(Ti_3Mo)	(Ti_3Nb)	(Ti_3W)	(Al_3Mo)	(Al_3Nb)	(Al_3W)
$D0_3$ (2)	−0.0362	−0.0253	0.0001	−0.0197	−0.0041	−0.0172	0.0120
	(Ti_3Al)	($TiMo_3$)	($TiNb_3$)	(TiW_3)	($AlMo_3$)	($AlNb_3$)	(AlW_3)
B11	0.0179	0.0254	0.0524	0.0464	0.0071	0.0328	0.0391
$C11_b$ (1)	0.0221	0.0594	0.0650	0.0597	0.0250	0.0292	0.0540
	($TiAl_2$)	(Ti_2Mo)	(Ti_2Nb)	(Ti_2W)	(Al_2Mo)	(Al_2Nb)	(Al_2W)
$C11_b$ (2)	−0.0039	0.0079	0.0548	0.0306	0.0165	0.0226	0.0518
	(Ti_2Al)	($TiMo_2$)	($TiNb_2$)	(TiW_2)	($AlMo_2$)	($AlNb_2$)	(AlW_2)

ordered compounds (table 3) (as the BCC structure is not close packed, we may expect the FP LMTO method, where the interstitial region is suitably treated, to be more precise).

The coherent-potential approximation (CPA) generalized perturbation (GP) method, within the tight-binding approach, gives the same tendency [16] (table 4); the formation energies of B2 and B32 are negative, and close to those found in the LMTO ASA investigation.

Table 3. Formation energies of the ordered compounds of Ti–Mo calculated using the LMTO methods.

	E_{for} (Ryd for two atoms)	
	FP LMTO results	LMTO ASA results
B2	−0.0161	−0.0188
B32	−0.0208	−0.0245
$D0_3$ (Ti_3Mo)	−0.0123	−0.0163
$D0_3$ ($TiMo_3$)	−0.0232	−0.0253

Table 4. Formation energies calculated by the tight-binding CPA GP method.

	E_{for} (Ryd for two atoms) Ti–Mo
B_2	−0.0180
B_{32}	−0.0270

In order to obtain some insight into the experimental situation of the Ti–Mo system, neutron diffraction measurements have been done by Caudron [17] on a polycrystal with 18% Mo at 800 °C. The result is in perfect agreement with the earlier work of Morniroli and Gantois. More precisely, we display, in figure 6, the diffuse intensity as a function of the modulus of the q-vector in reciprocal space. We see that there is a maximum diffuse intensity of a q-vector with a modulus equal to that of the family $\langle \frac{1}{2}\frac{1}{2}\frac{1}{2} \rangle$ (this is the only special point, with the same modulus, on the BCC lattice). This indicates, without ambiguity, a tendency to ordering (a tendency to segregation would have led to a maximum diffuse intensity at $q = \langle 000 \rangle$; this is definitely not the case). Moreover, the $q = \langle \frac{1}{2}\frac{1}{2}\frac{1}{2} \rangle$ wavevector corresponds precisely to the concentration wave of the B32 phase, which should be stable at low temperatures, according to our first-principles investigations.

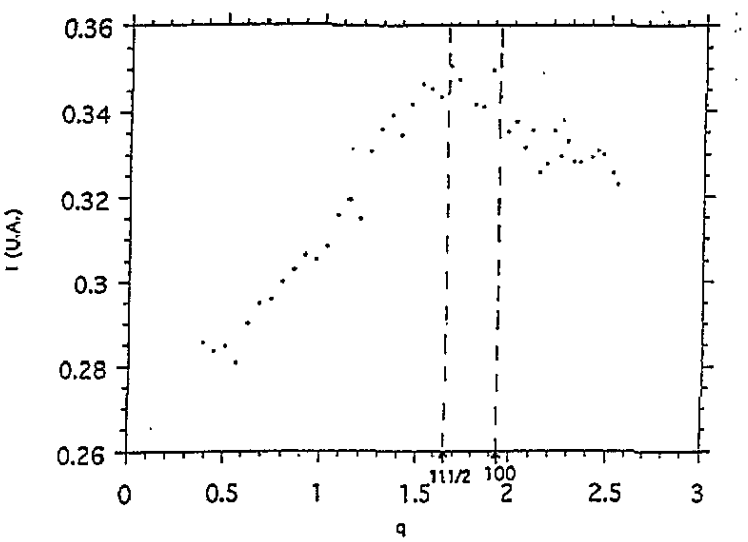

Figure 6. Diffuse intensity. Units: y axis, arbitrary units.

Hence, this result is interesting and confirms the validity of our LMTO ASA results (data for a single crystal are important to confirm this tendency to short-range order).

Now, we comment on the elastic relaxation effects. In the present first-principles calculations, the volume relaxation has been taken into account, but we neglected the internal relaxations of the cell. These internal relaxations may be important if the lattice mismatch between the pure elements and the different ordering phases is important. However, if we consider the crystalline parameters relative to the minima of the total energies, we can see that they are quite close to each other: 6.05 for the pure Ti element, 6 for Mo, 5.95 for B2, 6 for B32, 6 for $D0_3$ (Ti_3Mo), 5.95 for $D0_3$ ($TiMo_3$) (in units of Bohr radius a_0; see also figures 2 and 3(*b*)). Hence, we expect the elastic effects to be small. For the same reason, we have neglected the vibrational entropy term.

We now discuss the low-temperature regime. The experimental phase diagram (see figure 5(*a*)) indicates the existence of a two-phase regime between the HCP disordered phase (rich in Ti) and the BCC disordered phase (rich in Mo). When we estimated the formation energies of the ordered compounds of the Ti–Mo system, with respect to the HCP Ti and BCC Mo pure systems, we again found a tendency to ordering, in discrepancy with the experimental situation. We may conclude that all the results arising from electronic structure calculations are in conflict with the experimental phase diagram, which probably should be reconsidered.

3.2. The Ti–W system

The experimental phase diagram (see figure 5(*b*)) results from the early work of Rudy and Windisch [18], based on x-ray measurements. These workers showed the existence of a solid solution above 1250 °C. However, at 1100 °C, samples of alloys with 25 and 35% W have been studied and appeared heterogeneous. These workers concluded that there is a miscibility gap, and they estimated the concentrations of the two phases from the lattice parameter measurements. In fact, they have only proved the existence of a two-phase regime and not necessarily the presence of a miscibility gap, a two-phase regime between an ordered phase and a disordered phase is also possible.

We may conclude, as for the Ti–Mo system, that no direct experimental evidence exists concerning the presence, or not, of a miscibility gap for the BCC lattice.

For the low-temperature part of the diagram, the LMTO results are again in conflict with the experimental data.

If we consider the FP LMTO [16] and LMTO ASA results, we can see in table 5 that they are very close to each other, as for the Ti–Mo system.

Table 5. Formation energies of the ordered compounds of Ti–W calculated by the LMTO method.

	E_{for} (Ryd for two atoms)	
	FP LMTO results	LMTO ASA results
B_2	−0.0004	−0.0025
B_{32}	−0.0163	−0.0214
$D0_3$ (Ti_3W)	−0.0061	−0.0102
$D0_3$ (TiW_3)	−0.0174	−0.0197

The CPA GP results [16] are somewhat different, but still in favour of ordering.

Concerning the elastic relaxation effects, we note, as for the Ti–Mo system, that they are probably small. The crystalline parameters relative to the minima of the total energies

are very close to each over: 6.05 for Ti and 6 for W. The ordered compounds have identical crystalline parameters: 6 for B2, B32, $D0_3$ (Ti_3W), $D0_3$ (TiW_3) (in units of Bohr radius a_0; see also figures 2 and 3(*d*)).

Table 6. Correlation functions for the compounds.

	ξ_0	ξ_1	ξ_2	ξ_2'	ξ_3	ξ_4
Pure A	1	1	1	1	1	1
$D0_3$	1	0.5	0	0	−0.5	−1
B2	1	0	−1	1	0	1
B32	1	0	0	−1	0	1
$D0_3$	1	−0.5	0	0	0.5	−1
Pure B	1	−1	1	1	−1	1
$C11_b$ (1)	1	$\frac{1}{3}$	$-\frac{1}{3}$	$\frac{5}{9}$	$-\frac{1}{9}$	$-\frac{1}{3}$
B11	1	0	0	$\frac{1}{3}$	0	−1
$C11_b$ (2)	1	$-\frac{1}{3}$	$-\frac{1}{3}$	$\frac{5}{9}$	$\frac{1}{9}$	$-\frac{1}{3}$

Table 7. Interaction parameters for all the ternary systems calculated by the Connolly–Williams procedure.

Binary alloy	(Ryd for two atoms)					
	a_0	a_1	J_1	J_2	J_3	J_4
Ti–Al	−0.0252	0.0127	0.0076	−0.0012	−0.0011	−0.003
Ti–Mo	−0.0189	0.0045	0.0023	0.0025	−0.0004	0.0003
Ti–Nb	−0.0012	−0.0013	−0.0001	0.0006	0.0001	−0.0000
Ti–W	−0.0131	0.0047	0.0003	0.0034	−0.0004	0.0003
Al–Mo	−0.0114	0.0047	0.0006	0.0070	−0.0004	−0.0020
Al–Nb	−0.0078	0.0144	0.0024	0.0010	−0.0012	−0.0008
Al–W	0.0072	0.0067	−0.0035	0.0061	−0.0006	−0.0020

Table 8. Formation energies of the two $C11_b$ and B11 calculated by the Connolly–Williams procedure.

	E_{for} (Ryd for two atoms)						
	Ti–Al	Ti–Mo	Ti–Nb	Ti–W	Al–Mo	Al–Nb	Al–W
$C11_b$ (1)	−0.0312	−0.0165	−0.0006	−0.0064	0.0055	−0.0013	0.0289
B_{11}	−0.0246	−0.0183	−0.0006	−0.0116	0.0076	−0.0017	0.0248
$C11_b$ (2)	−0.0425	−0.0205	0.0006	−0.0011	0.0013	−0.0141	0.0230

3.3. Conclusions on Ti–Mo and Ti–W systems

All these results lead to some conclusions; the use of the LMTO ASA method on the BCC lattice is probably justified, because all the results are confirmed by the FP LMTO data. Concerning the Ti–Mo system, we may conclude that the experimental phase diagram is probably incorrect and that there is short-range order at high temperatures. We did not perform any experimental investigation for the Ti–W system, but our total-energy calculations indicate also a clear tendency to ordering in contradiction to the experimental phase diagram.

Table 9. Correlation functions for the ternary phases; see equation (5).

	1	c_{I}	c_{II}	$\langle p_{\mathrm{I}}^1 p_{\mathrm{I}}^3\rangle$	$\langle p_{\mathrm{I}}^1 p_{\mathrm{I}}^2\rangle$	$\langle p_{\mathrm{II}}^1 p_{\mathrm{II}}^3\rangle$	$\langle p_{\mathrm{II}}^1 p_{\mathrm{II}}^2\rangle$	$\langle p_{\mathrm{I}}^1 p_{\mathrm{II}}^3\rangle$	$\langle p_{\mathrm{I}}^1 p_{\mathrm{II}}^2\rangle$	$\langle p_{\mathrm{I}}^1 p_{\mathrm{I}}^2 p_{\mathrm{I}}^3\rangle$	$\langle p_{\mathrm{II}}^1 p_{\mathrm{II}}^2 p_{\mathrm{II}}^3\rangle$	$\langle p_{\mathrm{I}}^1 p_{\mathrm{I}}^2 p_{\mathrm{II}}^3\rangle$
A(Al)	1	1	0	1	1	0	0	0	0	1	0	0
B(Ti)	1	0	1	0	0	1	1	0	0	0	1	0
C(Nb)	1	0	0	0	0	0	0	0	0	0	0	0
B2(TiAl)	1	0.5	0.5	0	0.5	0	0.5	1	0	0	0	0.5
B2(TiNb)	1	0	0.5	0	0	0	0.5	0	0	0	0	0
B2(AlNb)	1	0.5	0	0	0.5	0	0	0	0	0	0	0
B32(TiAl)	1	0.5	0.5	0.25	0	0.25	0	0.5	1	0	0	0
B32(TiNb)	1	0	0.5	0	0	0.25	0	0	0	0	0	0
B32(AlNb)	1	0.5	0	0.25	0	0	0	0	0	0	0	0
$D0_3$ (Ti_3Al)	1	0.25	0.75	0	0	0.5	0.5	0.5	0.5	0	0.25	0
$D0_3$ (Al_3Ti)	1	0.75	0.25	0.5	0.5	0	0	0.5	0.5	0.25	0	0.25
$D0_3$ ($TiNb_3$)	1	0	0.25	0	0	0	0	0	0	0	0	0
$D0_3$ (Ti_3Nb)	1	0	0.75	0	0	0.5	0.5	0	0	0	0.25	0
$D0_3$ (Al_3Nb)	1	0.75	0	0.5	0.5	0	0	0	0	0.25	0	0
$D0_3$ ($AlNb_3$)	1	0.25	0	0	0	0	0	0	0	0	0	0
Heussler (Ti_2AlNb)	1	0.25	0.5	0	0	0	0.5	0.5	0	0	0	0
Heussler ($TiAl_2Nb$)	1	0.5	0.25	0	0.5	0	0	0.5	0	0	0	0.25
Heussler ($TiAlNb_2$)	1	0.25	0.25	0	0	0	0	0	0.5	0	0	0
$F\bar{4}3m$ (Ti_2AlNb)	1	0.25	0.5	0	0	0.25	0	0.25	0.5	0	0	0
$F\bar{4}3m$ ($TiAl_2Nb$)	1	0.5	0.25	0.25	0	0	0	0.25	0.5	0	0	0
$F\bar{4}3m$ ($TiAlNb_2$)	1	0.25	0.25	0	0	0	0	0.25	0	0	0	0

4. Cluster expansions using the Connolly–Williams procedure

We define now an Ising-like model, by labelling each site of the lattice by a pseudo-spin variable σ_n, which takes the value $+1$ or -1 depending or whether or not site n is occupied by an A species. Within this model, the formation energy ΔE_{i} of any configuration is written in terms of multisite interactions;

$$(\Delta E)_{\mathrm{i}} = \sum_{\alpha} J_\alpha (\xi_\alpha)_{\mathrm{i}} \tag{2}$$

where J_α is the cluster interaction associated with cluster α and $(\xi_\alpha)_{\mathrm{i}}$ the corresponding correlation functions in configuration i:

$$(\xi_\alpha)_{\mathrm{i}} = \Pi_{n\alpha}\sigma_n. \tag{3}$$

Of course, this cluster expansion is useful only of its converges fairly rapidly. In the spirit of a first-principles approach, the interactions J_α are calculated by inverting the set of equation (2), starting from the knowledge of a finite number of formation energies, as determined by the LMTO ASA method. Many applications [8, 9] of Ising-like theories to phase stability rely on this 'total-energy inversion method', also referred to as the Connolly–Williams method (for a review, see the last reference in [8]). We use here the Connolly–Williams method, with the interactions included into the irregular tetrahedron. We give in table 6 the correlation functions $(\xi_\alpha)_{\mathrm{i}}$, for each compound i.

When the space group symmetry is taken into account, equation (2) becomes

$$\Delta E = a_0\xi_0 + a_1\xi_1 + 4J_1\xi_2 + 3J_2\xi_2' + 12J_3\xi_3 + 6J_4\xi_4 \tag{4}$$

where ΔE is now the formation energy *per site* (ξ_1 is the joint correlation function; ξ_2 is the first neighbour pair correlation function; ξ_2' is the second neighbour pair correlation function;

Table 9. (continued)

$\langle p_{\mathrm{I}}^1 p_{\mathrm{II}}^2 p_{\mathrm{I}}^3 \rangle$	$\langle p_{\mathrm{II}}^1 p_{\mathrm{II}}^2 p_{\mathrm{I}}^3 \rangle$	$\langle p_{\mathrm{II}}^1 p_{\mathrm{I}}^2 p_{\mathrm{II}}^3 \rangle$	$\langle p_{\mathrm{I}}^1 p_{\mathrm{I}}^2 p_{\mathrm{I}}^3 p_{\mathrm{I}}^4 \rangle$	$\langle p_{\mathrm{II}}^1 p_{\mathrm{II}}^2 p_{\mathrm{II}}^3 p_{\mathrm{II}}^4 \rangle$	$\langle p_{\mathrm{I}}^1 p_{\mathrm{I}}^2 p_{\mathrm{I}}^3 p_{\mathrm{II}}^4 \rangle$	$\langle p_{\mathrm{I}}^1 p_{\mathrm{I}}^2 p_{\mathrm{II}}^3 p_{\mathrm{II}}^4 \rangle$	$\langle p_{\mathrm{I}}^1 p_{\mathrm{II}}^2 p_{\mathrm{I}}^3 p_{\mathrm{II}}^4 \rangle$	$\langle p_{\mathrm{II}}^1 p_{\mathrm{II}}^2 p_{\mathrm{II}}^3 p_{\mathrm{I}}^4 \rangle$
0	0	0	1	0	0	0	0	0
0	0	0	0	1	0	0	0	0
0	0	0	0	0	0	0	0	0
0	0.5	0	0	0	0	1	0	0
0	0	0	0	0	0	0	0	0
0	0	0	0	0	0	0	0	0
0.5	0	0.5	0	0	0	0	1	0
0	0	0	0	0	0	0	0	0
0	0	0	0	0	0	0	0	0
0	0.25	0.5	0	0	0	0	0	1
0.5	0	0	0	0	1	0	0	0
0	0	0	0	0	0	0	0	0
0	0	0	0	0	0	0	0	0
0	0	0	0	0	0	0	0	0
0	0	0	0	0	0	0	0	0
0	0.25	0	0	0	0	0	0	0
0	0	0	0	0	0	0	0	0
0	0	0	0	0	0	0	0	0
0	0	0.25	0	0	0	0	0	0
0.25	0	0	0	0	0	0	0	0
0	0	0	0	0	0	0	0	0

ξ_3 is the triplet correlation function; ξ_4 is the tetrahedron correlation function). The input of the inversion scheme is based on the formation energies of the following configurations: pure A, pure B, B2, B32 and the two $D0_3$ (see table 2). The results of the inversion scheme are presented in table 7 for all the binary systems. In order to test the reliability of the method, we have evaluated the formation energies, using the Connolly–Williams cluster interactions, of three extra structures: B_{11} and the two $C11_b$ (see figure 1 for the structures and table 8 for the results).

A comparison of tables 2 and 8 shows that the Connolly–Williams method does not reproduce the formation energies of phases not used in the inversion procedure. In fact, the $C11_b$ and B11 have positive formation energies, according to the total-energy calculations, and these energies cannot be reproduced conveniently through a Connolly–Williams procedure, based on structures with negative formation energies.

Hence, we have accepted applying the Connolly–Williams procedure without testing the transferability, as other workers have done in the recent past [19, 20]. This is a limitation, but one which is justified if we limit the use of the interaction parameters to the thermodynamic study of ordered compounds which have been precisely used for the inversion scheme.

5. Calculation of the phase diagram (isotherm) of the Ti–Al–Nb system

We want to use the Connolly–Williams inversion scheme to calculate the phase diagram (or the isothermal section) of a ternary system, using an appropriate configurational entropy.

Generally speaking, the formal expansion of the formation energy of a ternary systems contains some interaction parameters that do not appear in any binary expansion; these are the terms of the type $V_{\mathrm{A-B-C}}$; $V_{\mathrm{A-A-B-C}}, \ldots$. As a result, it is not possible simply to consider the binary expansions of the three binary systems (equation (4)) and to insert them into the ternary expansion, unless we set these extra interactions equal to zero (as

Table 10. Energies of the ternary compounds Heussler and $F\bar{4}3m$.

	Ti_2AlNb; Heussler	Ti_2AlNb; $F\bar{4}3m$	$TiAl_2Nb$; Heussler	$TiAl_2Nb$; $F\bar{4}3m$	$TiAlNb_2$; Heussler	$TiAlNb_2$; $F\bar{4}3m$
ΔE_{for} (Ryd for two atoms)	−0.0434	−0.0281	−0.0403	−0.0185	−0.0142	−0.0340

we did in an earlier publication [10]). The most natural way of dealing with the ternary alloy is simply to apply the Connolly–Williams procedure directly to the general form of the formation energy of a ternary system.

In the same spirit as in section 4, the internal energy of a ternary system is therefore written as, taking into account the space group symmetry of the BCC lattice,

$$\begin{aligned} E = \langle H \rangle = {} & a_0 + a_1 c_1 + a_2 c_{II} + 4(V_{I-I}^{1-3}\langle p_I^1 p_I^3\rangle + V_{II-II}^{1-3}\langle p_{II}^1 p_{II}^3\rangle + 2V_{I-II}^{1-3}\langle p_I^1 p_{II}^3\rangle) \\ & + 3(V_{I-I}^{1-2}\langle p_I^1 p_I^2\rangle + V_{II-II}^{1-2}\langle p_{II}^1 p_{II}^2\rangle + 2V_{I-II}^{1-2}\langle p_I^1 p_{II}^2\rangle) + 12(V_{I-I-I}^{1-2-3}\langle p_I^1 p_I^2 p_I^3\rangle \\ & + V_{II-II-II}^{1-2-3}\langle p_{II}^1 p_{II}^2 p_{II}^3\rangle + V_{I-I-II}^{1-2-3}\langle p_I^1 p_I^2 p_{II}^3\rangle + 2V_{I-II-I}^{1-2-3}\langle p_I^1 p_{II}^2 p_I^3\rangle \\ & + V_{II-II-I}^{1-2-3}\langle p_{II}^1 p_{II}^2 p_I^3\rangle + 2V_{II-I-II}^{1-2-3}\langle p_{II}^1 p_I^2 p_{II}^3\rangle) + 6(V_{I-I-I-I}^{1-2-3-4}\langle p_I^1 p_I^2 p_I^3 p_I^4\rangle \\ & + V_{II-II-II-II}^{1-2-3-4}\langle p_{II}^1 p_{II}^2 p_{II}^3 p_{II}^4\rangle + 4V_{I-I-I-II}^{1-2-3-4}\langle p_I^1 p_I^2 p_I^3 p_{II}^4\rangle + 2V_{I-I-II-II}^{1-2-3-4}\langle p_I^1 p_I^2 p_{II}^3 p_{II}^4\rangle \\ & + 4V_{I-II-I-II}^{1-2-3-4}\langle p_I^1 p_{II}^2 p_I^3 p_{II}^4\rangle + 4V_{II-II-II-I}^{1-2-3-4}\langle p_{II}^1 p_{II}^2 p_{II}^3 p_I^4\rangle). \end{aligned} \tag{5}$$

We have, for each site n, two independent occupation numbers, denoted p_I^n and p_{II}^n. p_I^n (or p_{II}^n) takes the value 1 or 0, depending or whether or not site n= 1, 2, 3 or 4 of the irregular tetrahedron is occupied by an A species (or a B species). In equation (5), the pairs 1–2 and 3–4 are second-neighbour pairs; the pairs 1–3, 1–4, 2–3 and 2–4 are first-neighbour pairs. The energy depends on 21 cluster interactions. For the inversion procedure, we consider the following 21 phases: the three pure elements; the three B2; the three B32; the six $D0_3$; the three ternary Heussler phases A_2BC, B_2AC and C_2AB; the three phases A_2BC, B_2AC and C_2AB with the symmetry $F\bar{4}3m$. The correlation functions of these 21 phases are presented in table 9.

We have applied this approach to the Ti–Al–Nb system. The formation energies of the three ternary Heussler phases and of the three $F\bar{4}3m$ phases are presented in table 10 (for the formation energies of the binary compounds, see table 2). The cluster interactions deduced from the inversion scheme are given in table 11.

Using these interactions, we have computed an isothermal section of the phase diagram of the Ti–Al–Nb system ($T = 1000\,°C$). The configurational entropy has been taken into account through the cluster variation method, within the irregular tetrahedron approximation. The result is presented in figure 7, together with the same isotherm calculated within a different approach and presented in an earlier publication [10]. The agreement between the two results give us some confidence in these two different approaches; despite their weaknesses (in the first approach in [10], the phase diagram of Ti–Al–Nb was computed using a phenomenological Hamiltonian whose parameters were obtained from knowledge of the three experimental binary phase diagrams).

6. Conclusions

The LMTO ASA calculations, presented here, give much interesting information on the alloys that we have considered. First, we have shown that the previously observed

Table 11. Cluster interaction parameters, for the Ti–Al–Nb system, calculated through the Connolly–Williams procedure using equation (6).

a_0 (Ryd for two atoms)	a_1 (Ryd for two atoms)	a_2 (Ryd for two atoms)	V^{1-3}_{I-I} (Ryd for two atoms)	V^{1-3}_{II-II} (Ryd for two atoms)	V^{1-3}_{I-II} (Ryd for two atoms)	V^{1-2}_{I-I} (Ryd for two atoms)	V^{1-2}_{II-II} (Ryd for two atoms)
0	−0.0688	0.0004	0.0185	−0.0034	−0.0085	0.0099	0.0007

V^{1-2}_{I-II} (Ryd for two atoms)	V^{1-2-3}_{I-I-I} (Ryd for two atoms)	$V^{1-2-3}_{II-II-II}$ (Ryd for two atoms)	V^{1-2-3}_{I-I-II} (Ryd for two atoms)	V^{1-2-3}_{I-II-I} (Ryd for two atoms)	$V^{1-2-3}_{II-II-I}$ (Ryd for two atoms)	$V^{1-2-3}_{II-I-II}$ (Ryd for two atoms)
0.0010	0.0038	0.0010	0.0043	0.0019	0.0021	0.0011

$V^{1-2-3-4}_{I-I-I-I}$ (Ryd for two atoms)	$V^{1-2-3-4}_{II-II-II-II}$ (Ryd for two atoms)	$V^{1-2-3-4}_{I-I-I-II}$ (Ryd for two atoms)	$V^{1-2-3-4}_{I-I-II-II}$ (Ryd for two atoms)	$V^{1-2-3-4}_{I-II-I-II}$ (Ryd for two atoms)	$V^{1-2-3-4}_{II-II-II-I}$ (Ryd for two atoms)
−0.0135	−0.0001	−0.0011	−0.0012	-0.0005	−0.0002

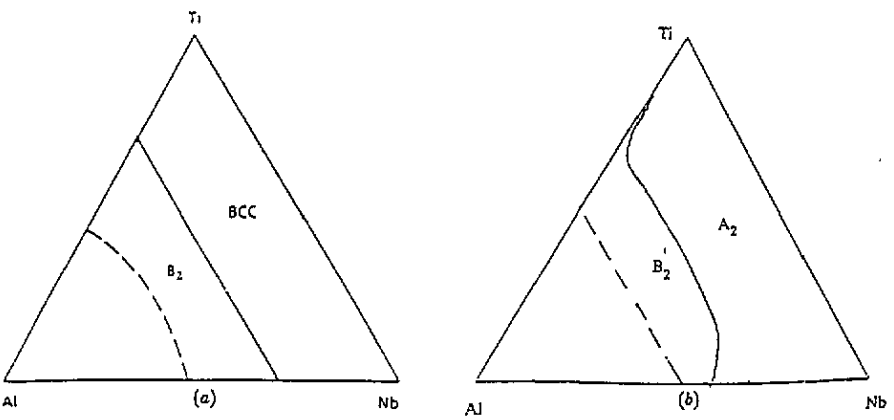

Figure 7. Isotherm of the Ti–Al–Nb system calculated from the Connolly–Williams method at 1000 °C: (*a*) from [10]; (*b*) from first-principles method.

segregation tendency of the Ti–Mo and Ti–W systems is in contradiction to our first-principles calculations, which predict ordering.

For Ti–Mo in particular, *in-situ* neutron diffraction measurements have been performed [17] and the results show that there is a well defined short-range order in the solid solution. This local order corresponds to a q-vector of the $\langle \frac{1}{2}\frac{1}{2}\frac{1}{2} \rangle$ type, in perfect agreement with our LMTO results, which predict the stability of the B32 phase.

Concerning the Ti–W system, we have seen that the reported experimental evidence for a miscibility gap is very indirect. Our LMTO investigations lead us to the same conclusions as for the Ti–Mo system, i.e. that there is a tendency to ordering. From this point of view, it should be very useful to perform *in-situ* neutron diffraction experiments to confirm this result.

Finally, applying the Connolly–Williams method to the total-energy calculations, and using a cluster variation method entropy, we have computed an isothermal section of the phase diagram of the ternary system Ti–Al–Nb. The agreement with the results obtained

previously [10] using a different approach is very good. In particular, we predict the stability of the B2 phase in a large domain of concentrations, and we do not find any segregation or two-phase regime in this system (this result seems to have been noticed already experimentally [21]). This shows that the Connolly–Williams method, when used cautiously, may lead to safe results.

Acknowledgments

The authors are very grateful to R Caudron and A Pasturel for very useful discussions and correspondence.

References

[1] Skriver H L 1991 *The L.M.T.O. Method* (Berlin: Springer)
[2] Yussouf M 1987 *Electronic Band Structure and its Applications (Lecture Notes in Physics 283)* ed M Yussouf (Berlin: Springer)
[3] Andersen O K 1975 *Phys. Rev.* B **12** 3060
[4] Andersen O K 1984 *The Electronic Structure of Complex Systems* ed W Temmerman and P Phariseau (New York: Plenum) p 10
[5] Hohenberg P and Kohn W 1964 *Phys. Rev.* B **136** 864
Kohn W and Sham L J 1965 *Phys. Rev.* A **140** 1133
[6] Skriver H L 1985 *Phys. Rev.* B **31** 1909
[7] Connolly J W and Williams A R 1983 *Phys. Rev.* B **27** 5169
[8] Lu Z W, Wei S H and Zunger A 1991 *Solid State Commun.* **78** 583
Lu Z W, Wei S H, Zunger A, Frota-Pessoa S and Ferreira L G 1991 *Phys. Rev.* B **44** 512
Zunger A 1995 *Statics and Dynamics of Alloy Phase Transformation (NATO ASI Series)* ed P E A Turchi and A Gonis (Dordrecht: Kluwer) at press
[9] Asta M, De Fontaine D and Van Schilfgaarde M 1995 *J. Mater. Res.* **8** 2554
[10] Rubin G and Finel A 1993 *J. Phys.: Condens. Matter* **5** 9105
[11] Murray J L 1987 *Phase Diagrams of Binary Titanium Alloys* (Metals Park, OH: America Society for Metals)
[12] Dupouy J M and Averbach B L 1965 *Acta Metall.* **9** 755
[13] Morniroli J P and Gantois M 1973 *Mem. Sci. Rev. Métall.* **70** 831
[14] Gros J P 1987 *Thèse de l'Institut National Polytechnique de Grenoble*
[15] Terauchi S *et al* 1978 *Proc. 2nd Int. Conf.* p 1335
[16] Pasturel A 1993 private communication
[17] Caudron R 1993 private communication
[18] Rudy E and Windisch St 1968 *Trans. AIME* **242** 953–4
[19] Tso N C and Sanchez J M 1989 *Superalloys, Superceramics and Supercomposites* ed J K Tien and T Caufield (New York: Academic) p 525
Tso N C, Kosugi M and Sanchez J M 1989 *Acta Metall.* **37** 121
Tso N C 1991 *PhD Thesis* Columbia University, New York
[20] Sluiter M and Turchi P E A 1989 *Phys. Rev.* B **40** 11215
[21] Naka S 1991 private communication